Arteriosclerosis, Thrombosis, and Vascular Biology

BRIEF REVIEW

Targeted Molecular Imaging of Cardiovascular Diseases by Iron Oxide Nanoparticles

Karla X. Vazquez-Prada, Jacinta Lam, Danielle Kamato, Zhi Ping Xu, Peter J. Little, Hang T. Ta

ABSTRACT: Cardiovascular disease is one of the major contributors to global disease burden. Atherosclerosis is an inflammatory process that involves the accumulation of lipids and fibrous elements in the large arteries, forming an atherosclerotic plaque. Rupture of unstable plaques leads to thrombosis that triggers life-threatening complications such as myocardial infarction. Current diagnostic methods are invasive as they require insertion of a catheter into the coronary artery. Molecular imaging techniques, such as magnetic resonance imaging, have been developed to image atherosclerotic plaques and thrombosis due to its high spatial resolution and safety. The sensitivity of magnetic resonance imaging can be improved with contrast agents, such as iron oxide nanoparticles. This review presents the most recent advances in atherosclerosis, thrombosis, and myocardial infarction molecular imaging using iron oxide-based nanoparticles. While some studies have shown their effectiveness, many are yet to undertake comprehensive testing of biocompatibility. There are still potential hazards to address and complications to diagnosis, therefore strategies for overcoming these challenges are required.

Key Words: atherosclerosis ■ cardiovascular diseases ■ magnetic resonance imaging ■ molecular imaging ■ thrombosis

Cardiovascular disease (CVD) is the leading cause of morbidity and mortality worldwide, with an estimated 31% of global deaths.[1] The underlying causes of mortality in CVD include heart attacks and strokes, which are caused by a vascular blockage that prevents blood from flowing to the heart or brain.[1–3] This is caused by the localized clotting of blood occurring in the arterial and venous circulation referred as thrombosis.[4]

Arterial thrombosis often results from thromboembolism or a complication of atherosclerosis, a multifactorial immunoinflammatory disease characterized by lesions in aortic tissue caused by LDL (low-density lipoprotein)-cholesterol retention to proteoglycans.[5] Macrophages uptake ox-LDL (oxidized LDL) and contribute to foam cell formation.[6] The death of these cells results in apoptotic cores full of thrombotic material. Rupture of unstable plaques releases these materials, activating the coagulation cascade and resulting in thrombus formation, which can lead to myocardial infarction (MI; Figure [A])[2,3,7,8] and an ischemic stroke.[9]

Venous thromboembolism can be divided into deep vein thrombosis and pulmonary embolism.[10] Deep vein thrombosis describes thrombus in the deep venous system (Figure [B]). The majority of deep-vein thrombi originate from thigh and lower leg veins. Pulmonary embolism occurs when a deep-vein thrombus detaches and reaches the lungs. The embolus subsequently impairs the gas exchange and circulation in the lung.[11] This causes ventilation-perfusion mis-match in the alveoli, and the activated platelets release serotonin and thromboxane.[12] These changes trigger vasoconstriction in the unaffected areas, increasing the pulmonary artery systolic pressure and right ventricular after load, leading to right ventricular failure.[10]

Thrombosis can range from an asymptomatic condition to a medical condition of swelling, edema, reddish discoloration and discomfort, which hampers a clinical evaluation and diagnosis based on symptomatology.[13] Symptoms of MI include chest pain, shortness of breath, and abnormal heart beating.[14] Atherosclerosis is asymptomatic in early stages until the plaques grow, and arterial lumen is reduced.[15] Early diagnosis and rapid treatment of CVDs is fundamental to decrease mortality and recurrence.[14] Diagnosis of CVDs is achieved by cardiovascular imaging using techniques like ultrasound, angiography, venography, optical coherence tomography,

Correspondence to: Hang T. Ta, School of Environment and Science, Griffith University, 170 Kessels Road, Brsbane 4111, Australia. Email h.ta@griffith.edu.au
For Sources of Funding and Disclosures, see page XXX.

Arterioscler Thromb Vasc Biol is available at www.ahajournals.org/journal/atvb

Nonstandard Abbreviations and Acronyms

CLIO	cross-linked iron oxide nanoparticles
CVD	cardiovascular disease
DCION2(+)	dual contrast iron oxide nanoparticles
EC	endothelial cell
EGFP-EGF1	fluorescent protein-epidermal growth factor 1
FibPeps	fibrin-binding peptides
HA-NWs	hyaluronan nanoworms
HUVEC	human endothelial umbilical vein cells
IONP	iron oxide nanoparticle
LDL	low-density lipoprotein
MCP-1	chemoattractant protein 1
MI	myocardial infarction
MRI	magnetic resonance imaging
ox-LDL	oxidized low-density lipoprotein
PEG	polyethylene glycol
PLGA	poly(lactic-co-glycolic acid)
RGO	reduced graphene oxide
ScFv	single-chain antibody
SPION	small supermagnetic iron oxide nanoparticle
USPIO	ultra-small supermagnetic iron oxide nanoparticle
VEGFR2	vascular endothelial growth factor receptor 2
VSMC	vascular smooth muscle cell

Highlights

- Current imaging methods to detect cardiovascular diseases such as atherosclerotic plaques and thrombosis are mostly invasive.
- Molecular imaging techniques have been developed as a noninvasive approach to image cardiovascular diseases due to its high spatial resolution and safety.
- A number of studies have shown the effectiveness of iron oxide as single- or multi-modality contrast agents in molecular imaging of atherosclerosis, thrombosis, and myocardial infarction.
- Targeting biomarkers on endothelial cells and vascular smooth muscle cells represents a promising strategy for the diagnosis of atherosclerosis while targeting activated platelets and fibrin is promising for thrombosis imaging.
- Many of the studies are yet to undertake comprehensive testing of biocompatibility. There are still potential hazards to address and complications to diagnosis, therefore, strategies for overcoming these challenges are required.

and computer tomography.[16] These techniques are associated with disadvantages such as invasiveness, the use of ionizing radiation and toxic contrasts that can cause side effects like nephropathies. Moreover, images can only be reconstructed for a selected phase of the cardiac cycle or have limited accuracy and specificity.[17,18]

Contrast agents could be labeled with targeting molecules that can specifically bind to biomarkers of the biological processes or disease sites, allowing low dose molecular imaging solutions and enhancing lesion detectability. Iron oxide nanoparticles (IONPs) have been widely studied and developed as imaging agents for diagnosis of diseases.[19–23] IONPs are also known as supermagnetic IONPs (SPIONs) because of their excellent magnetic applications.[24–28] SPIONs can alter the intrinsic contrast properties of biological tissues[1] directly by changing the proton density of a tissue, and[2] indirectly by altering the relaxation properties of surrounding hydrogen protons, changing local magnetic field or the resonance properties of a tissue and hence its relaxation time T_2 values.[16,24,29] In T_2-weighted imaging, the magnetic moments of unpaired electrons from the magnetic resonance imaging (MRI) contrast agents alter the local magnetic field strength, resulting in faster dephasing due to spin-spin effects, hence a shorter T_2 value. Relaxivity is a measure of the change in the relaxation rate of hydrogen protons as a function of contrast agent's concentration, and it is required to compare the efficacy of different IONPs as MRI contrast agents.[30] Here, we summarize the paramount findings in molecular imaging of atherosclerosis, thrombosis, and MI using IONPs as targeted contrast agents.

PASSIVELY TARGETED IONPS AS CONTRAST AGENTS FOR MOLECULAR IMAGING OF ATHEROSCLEROSIS AND THROMBOSIS

IONPs are eliminated by phagocytosis via the monocyte-macrophage system, suggesting they could accumulate where inflammatory responses are present, such as human atherosclerotic plaques and thrombi.[31] Studies in ApoE$^{-/-}$ mice demonstrate uptake of IONPs by macrophages. Macrophage uptake of citrate-coated IONPs was assessed at different stages of plaque development in the brachiocephalic artery.[32] Citrate-IONPs were injected 24 and 48 hours before the scans. Susceptibility gradient mapping MRI showed an increase of citrate-IONPs uptake with the progression of plaque development. Similar data were obtained from histology and mass spectroscopy analyses.

The coating of IONPs is of tremendous importance for the circulating time of the nanoparticles.[33] Generally, it was found that coating the nanomaterials with polyethylene glycol (PEG) shielded the surface from aggregation, opsonization, and phagocytosis,

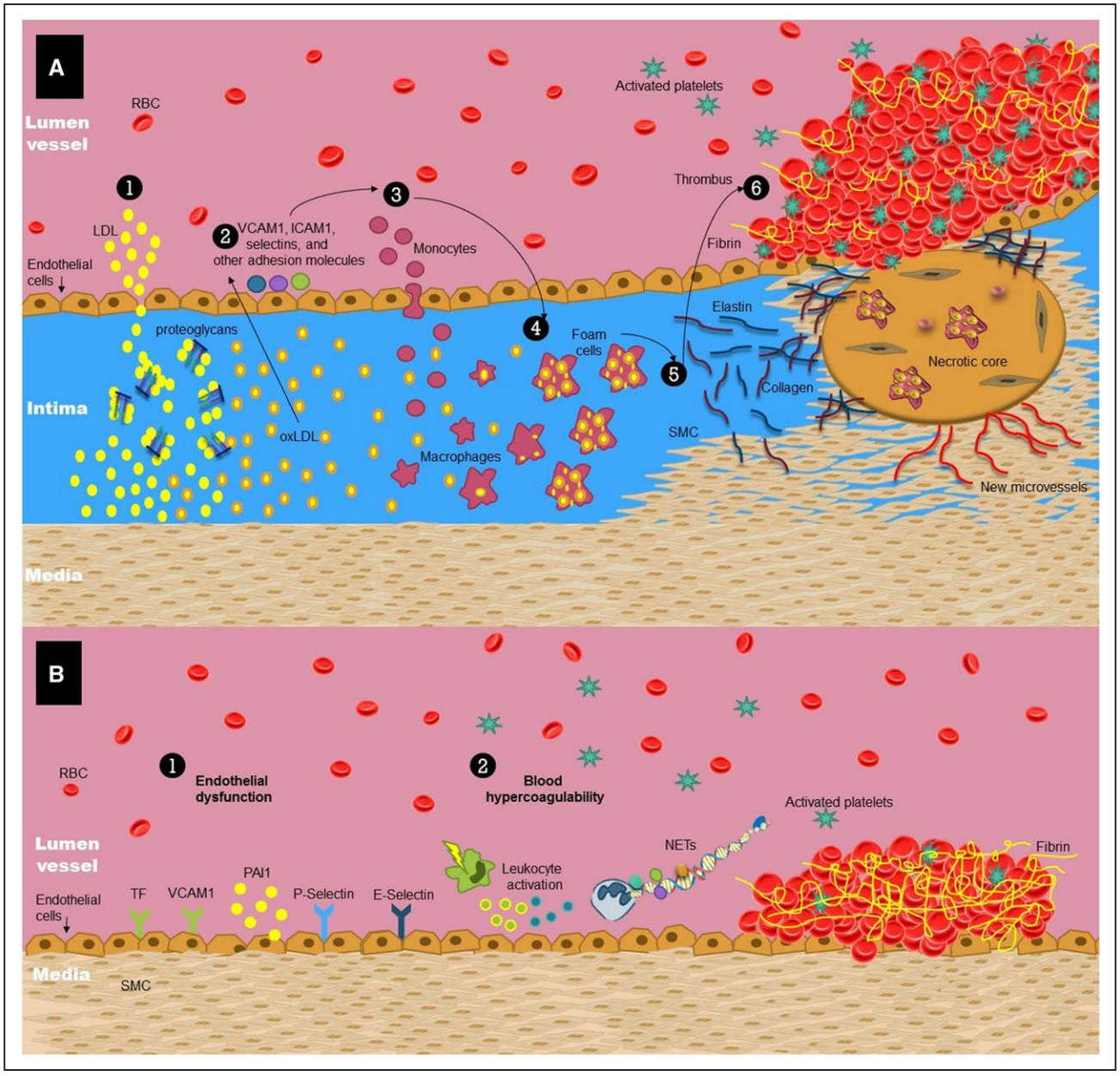

Figure. A, Development of atherothrombosis.
LDL (low-density lipoprotein)-cholesterol damages the endothelium and extravasates to the intima, accumulate in proteoglycans, and become oxidized.[1] Oxidation stimulates the endothelial cells (ECs) to produce adhesion molecules[2] that recruit monocytes.[3] M-CSF stimulates the differentiation of monocytes into macrophages that ex press SR-A and CD36. Macrophages recognize ox-LDLs (oxidized low-density lipoproteins) and phagocytize them, generating foam cells.[4] Smooth muscle cells may migrate to the intima and contribute to foam cells' formation.[5] The death of foam cells forms a mass of extracellular lipids and a fibrous cap of smooth muscle cell (SMC), collagen, and elastin. These lead to a necrotic and apoptotic core. If the plaque ruptures, the thrombogenic material is exposed to the lumen, platelets will activate, and adhere to the endothelium, forming a thrombus.[2,3,6–8] **B**, Development of venous thrombosis. Slow blood flow in the veins might lead to endothelial dysfunction and, therefore, expression of cell adhesion molecules such as VCAM1 (vascular cell adhesion protein 1), P-selectin, and E-selectin. This might lead to recruitment and activation of leukocytes to the vessel wall, downregulating antithrombotic factors, releasing neutrophil extracellular traps (NETs) upregulating inhibitor 1 (PAI1), and TF (tissue factor). These events trigger the coagulation cascade and accumulation of red blood cells and fibrin, blocking the vessel, and causing venous thrombosis.[13]

prolonging systemic circulation time of the materials.[34] Surprisingly, in the study of Ishida et al,[35] coating with PEG has shown to increase the accelerated blood clearance effect. In a murine model of peripheral arterial disease, PEGylated reduced-graphene oxide IONPs (reduced graphene oxide [RGO]-IONP-PEG) were used as carriers of ^{64}Cu, a radioisotope for positron emission tomography.[36] Positron emission tomography imaging was performed at longitudinally after inducing hindlimb ischemia in the mice. Animals were subdivided into mice that were used at each time point (naive group), and mice that were repeatedly injected

with the nanoparticles. Results showed effective accumulation of ^{64}Cu-RGO-IONP-PEG in the ischemic hindlimb at 24-hour postinjection. After 10 and 17 days postsurgery, the naive group showed prolonged blood pool uptake while the treated group rapidly cleared up the nanoparticles from circulation. In addition, the uptake of ^{64}Cu-RGO-IONP-PEG in the disease site was lower in reinjected mice, and there was higher liver uptake in the reinjected group compared with the naive group. The re-exposure of PEGylated RGO-IONP induces the accelerated blood clearance phenomenon and decreases the circulation half-life and passive targeting capabilities of ^{64}Cu-RGO-IONP-PEG. Hematoxylin and eosin staining revealed that the nanoparticles accumulated in the Kupffer cells and other phagocytic cells of the liver was much higher in the reinjected group. This is likely explained by the anti-PEG IgM and complement activation-mediated clearance of PEGylated nanomaterials. Production of anti-PEG IgM occurs in response to the injection of ^{64}Cu-RGO-IONP-PEG. When the mice were reinjected with the ^{64}Cu-RGO-IONP-PEG, the nanoparticles are quickly recognized by the anti-PEG IgM, resulting in complement activation and removal of the nanomaterials by the phagocytic system.

Another follow-up study[37] assessed the enhanced permeability and retention effect in peripheral arterial disease using a similar ischemia model. Positron emission tomography imaging showed that nanoparticle accumulation was the highest at day 3 and the lowest at day 17, while serial laser Doppler imaging showed that blood perfusion in the femoral artery decreased at day 3 and 10 but was improved at day 17 postsurgery. The nanoparticles accumulated in ischemic tissues via enhanced permeability and retention effect, which reduced as blood flow was normalized. These studies revealed that passive targeting of RGO-IONPs is a promising approach for multimodal imaging of CVDs.

ACTIVELY TARGETED IONPS FOR MOLECULAR IMAGING OF ATHEROSCLEROSIS, THROMBOSIS, AND MI

The surface of IONPs can be conjugated with ligands to enable site-specific interactions and enhance its delivery to the target of interest.[38] While passive targeting relies on the leakiness of blood vessels and passive diffusion, active targeting employs the attachment of binding ligands on the surface of the materials, allowing their specific binding to the surface markers of a target cell or tissue, improving specificity and efficiency of the contrast.[39] Recently, enormous progress has been made for targeting nanocarriers to improve therapeutic outcome and decrease systemic toxicity.

Targeting Monocytes/Macrophages With Dextran

Infiltration and accumulation of macrophages happen during the progression of atherosclerosis, thrombosis, and MI, making them a potential target for noninvasive techniques.[7,13] Targeting macrophages is often achieved by surface modification of IONPs with dextran, leveraging the expression of dextran-binding C-type lectins on the macrophage surface.[40]

Ferumoxytol is used for the treatment of anemia but has gained interest as contrast agent for MRI.[41] Yilmaz et al[41] evaluated whether ferumoxytol allows a better MRI characterization of infarct pathology than gadolinium-based agents in a clinical trial for 14 patients with acute MI. Baseline cardiac magnetic resonance was performed within 48 hours to 7 days after the cardiac symptoms. Patients in this study had acute ST-segment–elevationMI caused by coronary artery occlusion or plaque rupture and an ischemic cause of myocardial damage. Ferumoxytol was intravenously administered (17 mL ferumoxytol containing 510 mg Fe) 24 hours after the baseline cardiac magnetic resonance study. Then, patients underwent postferumoxytol studies 48 hours after ferumoxytol administration. Analyses suggest that ferumoxytol gave a more detailed analysis of MI mainly by macrophage infiltration and hence might provide a better profile for evaluating MI than Gd-based agents.

Sosnovik et al[42] showed that imaging of macrophages was possible in mice using magneto fluorescent nanoparticles (cross-linked iron oxide [CLIO]-Cy5.5) made of dextran-CLIO and Cy5.5. MI was induced by ligation of the left coronary artery in 12 mice, and sham surgery was performed in 7 mice as a control. CLIO-Cy5.5 were injected after surgery, and fluorescence tomography and MRI were performed 48-hour postinjection. MR images showed an increase in contrast-to-noise ratio in the infarcted mice (23.0±2.7), but not in the sham-operated mice (5.43±2.4). The fluorescence intensity of the infarcted mice (19.1±5.2) was greater than that of the control (5.3±1.4). CLIO have also been used as carriers of CyAm7[43] for detecting vulnerable atherosclerotic plaques with near-infrared fluorescence microscopy. CLIO-CyAm7 accumulated in the superficial intima and within plaque macrophages, endothelial cells (ECs), and SMCs with impaired endothelial barrier function, suggesting that vulnerable plaques exhibit impaired endothelial permeability, leading to higher nanoparticle uptake. Histology findings are also consistent with the uptake of CLIO-Cy5.5 by tissue macrophages as the excised hearts revealed the infiltration of inflammatory cells into the infarcted myocardium on hematoxylin and eosin staining.

Dextran-IONPs as carriers of iodine-125 for digital autoradiography of atherosclerotic plaques was also studied in ApoE$^{-/-}$ mice.[44] The nanoparticles

demonstrated high radiolabeling stability and long blood circulation time, leading to higher uptake in the heart of ApoE$^{-/-}$ mice compared with control. Digital autoradiography exhibited enhanced signals from the heart of ApoE$^{-/-}$ mice, peaking at 72 hours after administration of the nanoparticles.

Kao et al[45] used MCP-1 (monocyte chemoattractant protein 1) motif to coat spherical iron oxide magnetic nanoparticles and target monocytes in atherosclerotic plaques. MRI was performed in ApoE$^{-/-}$ mice 40-hour postadministration. In vivo images of the aorta showed an increase in the degree of darkness in mice fed with a high-fat diet for a longer time. A decrease of pixel density in nonfat fed mice of 25.4% and 26.5% (wild-type mice and ApoE$^{-/-}$ mice, respectively) was shown while a decrease of 38.1% and 40.9% ApoE$^{-/-}$ mice fed with high-fat diet for 2 and 4 days, respectively) was observed. Histology data confirmed that the kidney was the major organ employed for excreting the nanoparticles and that MCP-1-motif MNPs accumulated in vulnerable atherosclerotic plaques, indicating the potential affinity of MCP-1-motif MNPs in the atherosclerosis model.

Targeting Monocytes/Macrophages With Other Moieties

Active targeting of macrophages can be accomplished by conjugation with osteopontin targeting agents. Osteopontin is overexpressed by foamy macrophages in atherosclerotic plaques.[46] Qiao et al[47] developed Cy5.5-labeled osteopontin antibody-DMSA-coated IONPs (Cy5.5-OPN-DMSA-IONPs) for MRI/optical dual-modality imaging. Hematoxylin and eosin, Masson trichrome, and immunofluorescence staining revealed the expression of OPN in atherosclerotic plaques. These nanoparticles enhanced T_2 contrast in vivo in ApoE$^{-/-}$ mice with a mean post/presignal ratio of 0.64 compared with the control.

Tenascin-C, highly expressed in monocytes and macrophages, leads to inflammation and plaque rupture.[48] Li et al[49] developed antitenascin-C antibody ultra-small supermagnetic iron oxide nanoparticles (USPIOs) for evaluating the vulnerability of atherosclerotic plaques in ApoE$^{-/-}$ mice. Mice were either injected with antitenascin-C USPIO or with nontargeted USPIO. The MR images were taken before injection and after 16 and 24 weeks. At 16 weeks, the relative signal intensity in the targeted group was reduced by 15.7% which was more than that of the control group (reduced by 3.4%). Similar results were seen at 24 weeks, where the relative signal intensity changes in the targeted and the control group were −26.4% and −11.1%, respectively. Histopathologic analyses demonstrated atherosclerotic plaque formation and confirmed that tenascin-C expression of the plaques at 24 weeks was higher than that at 16 weeks (0.22 ± 0.04 versus 0.13 ± 0.02, $P < 0.05$).

Hyaluronan is an endogenous ligand for CD44, an adhesion protein expressed on cells involved in atherosclerosis such as macrophages.[50] The effect of the morphology of hyaluronan-conjugated iron oxide nanoworms (HA-NWs) and hyaluronan-conjugated SPIONs (HA-SPIONs) on inflammatory responses of atherosclerotic plaques was studied in ApoE$^{-/-}$ mice.[51] HA-NW has an elongated shape whereas HA-SPIONs is a spherical. The mice were injected with HA-SPIONs and HA-NWs, and T_2*-weighted images were obtained before and postinjection. Administration of HA-NW caused T_2* signal intensity of the aorta wall to reduce by 20% of preinjection levels at 20 minutes after injection and this effect was sustained for over 120 minutes. HA-SPIONs caused significant MR signal losses and the intensities of lumen did not recover even after 140 minutes, preventing the detection of plaques on aorta walls due to a lack of MR contrasts between the lumen and aorta walls. The result indicated that nanomaterial shape is important for targeting to blood vessel wall, which is consistent with other reports.[52] HA-NWs were less toxic as shown by lower cytokine levels in RAW 364.7 cells, probably because low molecular weight HA can produce inflammatory responses, while the high molecular weight HA are anti-inflammatory. CD44 binding affinity to HA is dependent on the molecular weight and it significantly increases with higher molecular weight of HA. Considering that one nanoworm consists of multiple SPIONs, it is possible that the elongated structure of the SPIONs arranged together can better mimic high molecular weight HA and reduce the inflammatory responses generated by the iron oxide core of the nanoprobes. These results indicate that HA-NWs were not only safer, but also more superior imaging agents than HA-SPIONs.

CD163 is a membrane receptor expressed by macrophages and is associated with plaque progression in atherosclerotic lesions. CD163-targeted gold-coated-IONPs were tested as contrast agents for detection of atherosclerotic plaques in ApoE$^{-/-}$ mice.[53] Imunohistochemistry validation confirmed all the mice had atherosclerotic lesions in the MRI scanned area and that the plaques were composed by a layer of smooth muscle cells with small lipid deposits and infiltrated macrophages. MRI was performed before and after administration. The MR images showed a decrease in T_2 signal at 24 hours, which became significant at 48 hours, providing evidence that the nanoparticles were able to enhance the visualization of atherosclerotic plaques and their targeting of macrophages with CD163 was successful.

Annexin V is used to target apoptotic macrophages in vulnerable plaques, as it binds to phosphatidylserine.[54] Cheng et al[55] reported a hybrid-nanosystem for imaging using a single-photon-emission computed tomography/MRI multimodal probe. The nanosystem consisted of PEG-USPIOs functionalized with diethylenetriaminepentacetate acid for (99 m)Tc coordination and annexin

V (99mTc—DTPA—USPIO—annexin V) for targeting purposes. Single-photon-emission computed tomography and MRI images in mice were consistent and showed an accumulation of the probes in vulnerable atherosclerotic plaques. Absorption of 99mTc—DTPA—USPIO—annexin V by apoptotic macrophages lead to an enhancement of T_2-weighted MRI. A signal change of atherosclerotic plaques can be observed at 8-hour postinjection. Lesions in the aorta can be outlined when integrated with the MR images taken before the injection, improving the focal localization, and volumetry of atherosclerotic plaques. Moreover, radioactive signals detected by single-photon-emission computed tomography facilitated focus recognition and quantification of vulnerable atherosclerotic plaques. Targeting effects were further confirmed by CD-68 and transferase dUTP nick end labeling staining. Results suggest that the annexin V-modified hybrid nanoparticle system specifically targeted the vulnerable atherosclerotic plaques containing apoptotic macrophages.

Mannose receptors are overexpressed in some activated macrophages in rupture-prone atherosclerotic plaques and can potentially be used for effective targeting.[56] Babič et al[57] tested different nanoparticles (Resovist, γ-Fe_2O_3, and γ-Fe_2O_3) coated with either D-mannose or poly(L-lysine). In vitro MRI showed an increase in relaxivity after incubating the macrophages in nanoparticle-containing medium for 3 hours, which continued to increase until 24 hours. Intraperitoneal injection with D-mannose and poly(L-lysine)-γ-Fe_2O_3 nanoparticles in Prague hereditary hypercholesterolemic rats exhibited signal loss in the abdominal cavity immediately but disappeared 24 hours after administration. Even though viability and relaxivity of both nanoparticles were similar, poly(L-lysine)-γ-Fe_2O_3 nanoparticles were considered optimal, as the D-mannose might be more easily metabolized, exposing the uncoated iron oxide cores to the cell environment.

Targeting Endothelial Cells

ECs constitute one of the essential components of the circulatory system and thus are an important element to consider for targeting CVDs. E-selectin, an adhesion protein expressed only on ECs activated by cytokines, was used to target ECs.[58] CLIO nanoparticles were conjugated with an anti-human E-selectin (CD62E) F(ab')$_2$ fragment to form CLIO-F(ab')$_2$. Feasibility of CLIO-F(ab')$_2$ as MRI endothelial proinflammatory markers in vitro using human endothelial umbilical vein cells (HUVEC) was assessed. HUVECs were implanted in athymic mice in matrigel solution and were treated with IL-1β (interleukin-1β) and to express E-selectin. The formation of HUVEC-containing vessels was confirmed by histology and microscopy. Vessels that were highly positively stained for iron were detected only in matrigel implants initially seeded with HUVECs. Treated HUVECs showed 100 to 200× higher binding to the nanoparticles than control cells. MRI showed that the cells treated with IL-1β also had a specific T_2-weighted signal darkening, suggesting that the system could be of potential use in monitoring diseases such as atherosclerosis.

Ex vivo MRI of CLIO-F(ab')$_2$ was tested using a model of HUVEC transfer to test specific imaging probes for human vascular disease.[59] Animals harbouring HUVEC-containing matrigel implants and blank matrigel implants were euthanized longitudinally after implantation. The implants were dissected without perfusion and analyzed by histology and microscopy. Immunohistochemical staining for VEGFR2 (vascular endothelial growth factor receptor 2) and CD31 indicated the successful and specific conjunction of anti-VEGFR2 antibodies onto the nanoparticles. The CLIO-F(ab')$_2$ were injected following the induction of E-selectin expression with IL-1β and hypointensity was found only if treated with the interleukin. MRI images were taken preinjection and postinjection of CLIO-F(ab')$_2$. Analyses showed a 3-fold decrease in T2* images measured in HUVEC implants in response to IL-1β treatment. These observations support the in vitro findings and suggest that IL-1β-induced E-selectin expression in this HUVEC model is detectable by MRI using CLIO-F(ab')$_2$.

VEGFR2 stimulates neoangiogenesis, which promotes infiltration of macrophages, thickening of the vessel wall, deposition of lipids, inflammation, atherosclerotic plaque progression, and rupture.[60] A nanosystem consisting of VEGFR2-targeted perfluorocarbon magnetic nanocapsules was designed for dual-modality imaging of atherosclerotic neovasculature.[61] In the study, perfluorooctyl bromide was used as an ultrasound contrast agent. Ultrasound imaging was performed before and after injecting the nanocapsules in atherosclerotic rats. MR images were obtained before and postinjection. Ultrasound images showed echogenicity in the atherosclerotic/targeted group (65.1 dB) but not in the atherosclerotic/nontargeted (46.7 dB) or control/targeted group (46.0 dB). Similarly, the nanocapsules significantly attenuated the MRI contrast-to-noise ratio in the atherosclerotic/targeted group (74.2) but not in the atherosclerotic/nontargeted (48.9) or control/targeted group (46.9).

Targeting VSMCs

Vascular smooth muscle cell (VSMCs) are another component of the vascular wall with a key role in the progression of many CVDs. Targeting VSMCs can be achieved by targeting profilin-1, an actin-binding protein that regulates VSMCs' proliferation and migration. Notably, its overexpression can lead to atherosclerosis.[62] Profilin-1 targeted IONPs (PC-NPs) were synthesized for MR and fluorescence dual-modality imaging.[63] In vivo MR and

near-infrared fluorescence imaging were performed in ApoE$^{-/-}$ mice before and 36 hours after administration of nanoparticles. Compared with the nontargeted group, the fluorescence signal of the carotid artery was significantly higher in the targeted group. Similarly, the T_2 signal was significantly attenuated 36-hour postinjection, and the contrast to noise ratio was significantly reduced in the targeted group (31.7%) compared with the nontargeted group (9.47%). Histology verification showed more nanoparticles deposited in atherosclerotic lesions of targeted group than those in other groups.

Targeting Activated Platelets

Platelets contribute to not only thrombus formation, but also the inflammatory processes that affect atherosclerotic plaque development.[12] Targeting activated platelets for molecular imaging was explored by Ta et al.[29,64–66] They developed a 2-step chemoenzymatic coupling method for site-specific conjugation of a single-chain antibody (scFv) against LIBS epitopes on glycoprotein IIb/IIIa. In vitro adhesion assays and in vivo experiments in C57BL/6 wild-type mice suggest that the scFv was successfully conjugated to the particles. Flow cytometry assays confirmed the specific binding of scFv to activated platelets and nonbinding to nonactivated platelets. Furthermore, there was an enhancement in T2*-weighed images for the detection of thrombosis in mice. Histological analysis of the injured carotid artery demonstrated MPIOs that bound on the induced thrombus.

Multimodal IONPs for targeted MRI of atherothrombosis was developed recently.[16] The dual contrast IONPs (DCION2[+]) acted as positive and negative contrast agents. DCION2(+) were functionalized with scFv directed against activated platelets for molecular MRI and labeled with fluorescent molecules for optical imaging purposes. The targeting of DCION2(+) to activated GPIIb/IIIa receptors was demonstrated in vitro with receptor-expressing CHO cells and with activated platelets. Results show that DCION2(+) were able to shorten both T_1- and T_2-relaxation times. MR imaging of the thrombi in vitro showed contrast in T_1- and T_2-weighted imaging and demonstrated the efficient binding of DCION2(+) on the thrombi. The dual contrast was shown by a bright ring around the thrombi in T_1-weighted images and by a dark ring around the thrombi in T_2-weighted images. In vivo MRI showed the largest change in signal at 70-minute postinjection and a gradual decline after this time point. Ex vivo fluorescence imaging confirmed the specific binding of DCION2(+) to thrombus.

Versatile ultra-small super-paramagnetic nanoparticles differ from SPIONs by its functionalization with aminated polysiloxane film grafted on their surface and embedded in a dextran corona. versatile ultra-small super-paramagnetic nanoparticles were functionalized with recombinant human IgG4 antibody (rIgG4 TEG4) to target platelet membrane glycoproteins αIIB and β3.[67] Staining of macrophages by anti-CD68 antibody was performed to show the localization of platelets. Results show an accumulation of nanoparticles in areas of foam cells and platelet-leucocytes-aggregates. Transversal relaxivity of the nanoparticles was found to be 273 mmol/L^{-1} s^{-1} in the presence of platelets and 257 mmol/L^{-1} s^{-1} when measured alone. Ex vivo MRI of the aorta of mice injected with the TEG4-versatile ultra-small superparamagnetic nanoparticle showed a selective binding of TEG4-versatile ultra-small super-paramagnetic nanoparticle on atheroma plaques which induced a loss of MRI signal, whereas no loss of signal was observed in mice injected with IgG-USPIOs.

Another platelet-targeting IONPs were coated with fucoidan (USPIO-FUCO), a sulphated polysaccharide having high affinity for P-selectin.[68] Suzuki et al[69] synthesized USPIO-FUCO and found that the nanoparticles bound to P-selectin in vitro. In vivo thrombi could be evidenced by MRI on animals injected with the USPIO-FUCO. Importantly, there was no variation in signal postinjection with control USPIO nanoparticles after 2 hours. MRI of thrombi were correlated with P-selectin immunostaining and USPIO detection by electron microscopy. Data suggest that an effective targeting to activated platelets was achieved in in vivo MRI thrombi imaging.

Arg-Gly-Asp (RGD) domain is a cell adhesion motif present in many integrins and matrix molecules, including GIIb/GIIIa.[70] Targeting activated platelets through GIIb/GIIIa with cRGD conjugated PLGA-IONPs for detection of thrombosis was reported.[71] The PLGA-IONPs-cRGD were tested in vivo using a rat model of $FeCl_3$-induced abdominal aorta thrombosis. In vivo and ex vivo biodistribution indicated that the nanoparticles accumulated selectively on the surface of the thrombi and were internalized by macrophages in the liver and the spleen. Moreover, in vivo MRI data showed a decrease in T_2 signal at the thrombus 10 minutes after injection and a gradual increase until 50 minutes, suggesting that this nanosystem might represent a promising contrast agent for specific detection of thrombosis.

Fusion proteins such as EGFP-EGF1 (enhanced green fluorescent protein-epidermal growth factor 1) have recently gained interest as they can be conjugated in nanomaterials with the purpose of providing targeting moieties and contrast ability. EGF1 binds to the tissue factor present in activated platelets whereas EGFP provides fluorescence. Hu et al[72] synthesized EGFP-EGF1 to target activated platelets for dual molecular imaging of cerebral thrombosis.[72] In vivo multispectral fluorescence imaging validated the targeting efficiency of EGFP-EGF1-IONPs. The nanoparticles were mainly accumulated in the tissue factor exposure region of the brain, suggesting EGFP-EGF1-IONPs might be a feasible contrast agent for the early diagnosis of cerebral thrombosis.

Although the authors did not present any data of MRI studies, it might be worth conducting MRI analyses in a follow-up study, as the nanosystem is based on IONPs, which are known to be contrast agents for MRI.

Targeting Fibrin

Fibrin is a key component of thrombi and a crucial factor in atherosclerosis.[73] An IONP-micelle system was functionalized with FibPeps (fibrin-binding peptides) for the detection of thrombi.[74] Thrombus detection by FibPep-ION-Micelles was studied in a mouse model of carotid artery thrombosis with in vivo quantitative MRI. Histological analysis confirmed the occlusion of the injured carotid arteries and the absence of occlusion in the contralateral, noninjured carotid arteries. Thrombus uptake of FibPep-ION-Micelles and measurements of the carotid arteries were performed ex vivo using a magnetic particle spectrometer. FibPep-ION-Micelles showed decreased T_2 value in the thrombus area (22.7±1.5 ms) in comparison with the preinjection value (26.5±2.6 ms). Ex vivo magnetic particle spectrometer confirmed an increased thrombus signal compared with the noninjured control. In contrast, there was no increase in magnetic particle spectrometer thrombus signal for the FibPep-ION-Micelles when compared with the nontargeted micelles, suggesting the uptake of the nanoparticles by the thrombi might be due to entrapment. Thus nontargeted ION-Micelles might be of value for diagnosis of thrombosis.

One of the peptide molecules used to target fibrin is CREKA due to its interactions with fibrin-fibronectin complexes.[75] Spherical hybrid metal oxide-peptide amphiphile micelles were developed for molecular MRI of human clots.[76] The micelles consisted of an iron oxide core and were functionalized with fibrin-targeting peptide amphiphiles with the sequence CREKA. Studies with in vitro clots showed that the signal intensity of MR images with targeted micelles was 65% compared with 35% for nontargeted, exhibiting a 2-fold T_2 signal enhancement.

Ta et al[77,78] designed a MRI nanosensor to distinguish age of thrombus. The nanosensor consisted of IONPs coated with a detachable layer of Gd and functionalized with peptide targeting fibrin, which is present on both fresh and old thrombi. If the nanosensor binds to a fresh thrombus, thrombin (present only in fresh thrombus) will release the Gd from the IONPs, restoring T_1 signal. On the contrary, if the thrombus is old it will remain intact and it will possess T_2 signal. Results show that the absence of thrombin generated low r_1 values while in the presence of thrombin, r_1 increased significantly. In addition, the absence of thrombin exhibited high r_2 values, showing that IONPs are useful not only to detect thrombi, but also to estimate its age.

In summary, these studies demonstrate that IONPs can be functionalized with ligands to target different features of atherosclerotic plaques and thrombotic events, including VSMCs, ECs, monocytes, macrophages, platelets, and fibrin. The targeted IONPs successfully accumulate in the region of interest and can enhance MR images by significantly inducing contrast.

IN VITRO AND IN VIVO TOXICITY OF IONPs

IONPs are the most used nanoparticles for biomedical purposes, including the diagnosis of disease. Nonetheless, the understanding of their interactions with biological systems, toxicity, and uptake mechanisms is limited and is a field of major interest. The toxicity and biocompatibility of most of the nanoparticles reviewed above has been assessed in vitro and in vivo.

Murine 4T1 breast cancer cells were used to test in vitro toxicity of passive-targeted RGO–IONP–PEG using the MTT assay. The cells were incubated for 24 hours with different concentrations of RGO–IONP–PEG, and no obvious toxicity was seen. Reactive oxygen species were measured by dichlorodihydrofluorescein diacetate staining and used as an indicator of oxidative stress in RGO–IONP–PEG incubated cells. Results showed no generation of reactive oxygen species even at the highest concentration tested (200 $\mu g \cdot mL^{-1}$). Moreover, mice treated with RGO–IONP–PEG (200 µL, 2 $mg \cdot mL^{-1}$) after photothermal therapy survived over a period of 40 days without a single death, showing no sign of toxicity nor significant body weight loss.[79] Histological examination of major organs showed no apparent damage or abnormality, suggesting that RGO–IONP–PEG was not toxic to mice with these concentrations. On the contrary, other studies suggest that RGO may have potential interaction with serum proteins and induce intracellular reactive oxygen species, which has limited the clinical translation of this nanoplatform.[36]

Cytotoxicity of dextran-IONPs such as ferumoxytol and ferucarbotran has been assessed in vitro.[41] Incubation of macrophages for 24 hours with ferumoxytol (0.5 mg Fe/mL) and the lower concentration ferucarbotran (0.25 mg Fe/mL) did not result in significant morphological changes and was not toxic, whereas incubation with higher concentration ferucarbotran (0.5 mg Fe/mL) resulted in rapid cell death. Biodistribution study of dextran-IONPs as carriers of iodine-125 targeting mouse atherosclerotic plaques (100 µL, 10 µCi, 0.2 mg Fe/mL) show that the nanoparticles remained in the site while they were cleared in the healthy tissues.[44] MCP-1 magnetic nanoparticles viability assays (0.1, 0.2, and 0.3 mg Fe/mL culture medium) also show that these dextran-IONPs do not affect the viability of monocytes and 3T3 cells.[45]

Toxicity and biocompatibility studies of IONPs targeting monocytes-macrophages with other moieties yielded similar results as dextran-IONPs.

Cy5.5-OPN-DMSA-IONPs had low cytotoxicity from 5 to 50 µg/mL on 265.7 macrophages. Additionally, terminal deoxynucleotidyl transferase dUTP nick end labeling and flow cytometry assays showed that the nanoprobes had insignificant influence on the apoptosis of macrophages.[47] CellTiter 96 AQueous one solution cell proliferation assay (MTS) suggested that HA-NWs (0.0625, 0.125, 0.25, 0.5, 1 mg/mL) did not affect viability of vascular endothelial EA.hy926 cells. Furthermore, biocompatibility and histopathologic analysis performed postinjection (8 mg Fe/kg) of the nanowires did not show any signs of toxicity on mouse major organs.[51]

MTT assays of IONPs targeting VSMCs through profilin-1 showed no significant effect on VSMCs and macrophage viability after 24 hours incubation, even at concentrations as high as 0.5 mg/mL.[63] Promising results have been obtained from toxicity assays performed with activated platelet targeted IONPs.[71,72] In vivo toxicity studies of Fe_3O_4-PLGA-cRGD in rats (1 mL, 1 mg/mL) obtained no evident effect on blood composition, liver, or kidney function postinjection.[71] In vitro cytotoxicity of EGFP-EGF1-IONPs was determined using CCK-8 assay on U87MG cells and HUVECs. Results suggest that there was no obvious cytotoxicity on both cell types in the studied concentration range (protein or iron 0–50 µg/mL).[80]

In vitro and in vivo studies reviewed herein provide evidence that IONPs were well-tolerated by a variety of cell lines and were, therefore, nontoxic under conditions tested. However, other targeted IONPs should also be investigated to ensure safety and further studies are needed to evaluate long-term effects.

CONCLUSIONS AND PERSPECTIVES

The unique properties of IONPs such as paramagnetism, high surface-to-volume ratio, and biocompatibility has led to extensive research for biomedical applications. This review presented the most recent advances in the molecular imaging of atherosclerosis, thrombosis, and MI using IONPs (Table). Overall, IONPs reviewed are nontoxic under conditions tested and have been conjugated with different probes to develop single or bimodal contrast agents for molecular imaging. Most of the research on IONPs as contrast agents has been focused on MRI. The relaxivity of IONPs critically depends on size, shape, and coating. The IONPs discussed had a size range of 6 to 404.4 nm and a r_2 and r_1 range of 20.1 to 489 mmol/$L^{-1}s^{-1}$ and 5.3 to 44.6 mmol/$L^{-1}s^{-1}$, respectively.

Comparing different IONPs has proved to be challenging in this review as not all studies have provided data on the relaxivity of the nanoparticles. While most studies provided information about the signal change, different measures were used, including post/presignal ratio, relative signal intensity change, contrast to noise ratio, and signal brightness intensity. Therefore, as more novel IONPs are developed, it is important that researchers provide these data with a qualitative and standardized measurement of signal intensity change.

Most of the IONPs have been designed to target the monocyte-macrophage system, either passively or by targeting macrophages with dextran, D-mannose, poly(L-lysine), and antibodies. There are concerns of misleading diagnosis in the clinic since macrophages will localize to most inflammatory responses within the body, which could be reduced by the development of IONPs with dual targeting systems to improve the targeting efficacy. Studies reviewed have shown that targeting ECs through E-selectin and VEGFR2, as well as targeting VSMCs via profilin-1 represent promising strategies for the diagnosis of atherosclerosis. Moreover, activated platelets and fibrin are the most common target markers for thrombosis. Activated platelets have shown to be targeted either through glycoproteins with peptides (RGD) or antibodies (scFv and anti-IgG4), or through other proteins such as P-selectin and tissue factor with fucoidan and EGF, respectively. Peptides targeting fibrin include CREKA and FibPeps. Activated platelets and fibrin have demonstrated to not only be promising targets to diagnose thrombosis but also rate the degree and the age of thrombus, making it easier for clinicians to provide the correct treatment for each patient.

Within the clinical landscape of IONPs used for MRI, the only active IONPs currently being used as MRI contrast agent for the cardiovascular system is ferumoxtran-10.[81,82] Ferumoxides and ferucarbotran were designed for MRI of the liver but have also been tested as cardiovascular MRI contrast agents. Ferumoxides caused severe back pain during administration and was discontinued in 2008.[82] Ferucarbotran was discontinued in 2009 because its enhancement was less efficient than gadolinium-based agents.[83] Ferumoxytol is currently used for treatment of anemia and under ongoing Food and Drug Administration clinical trials for an alternative contrast medium for MRI. Despite the label change and the Food and Drug Administration's boxed warning added to the Feraheme (ferumoxytol) label in March 2015, radiologists have shown increasing interest in using ferumoxytol as a supplement or alternative to gadolinium. Recent clinical trials data suggest ferumoxytol is a safe and promising contrast agent for MRI, especially for imaging the nervous and the cardiovascular system.[84] Serious adverse events appear to be rare. With proper precautions, ferumoxytol may be a valuable MRI agent.

While some studies have shown their effectiveness as contrast agents in molecular imaging, many of the studies are yet to undertake in vivo or in vitro testing for biocompatibility. There are potential hazards and complications to address. The potential impact of accumulation of these agents in tissues and their elimination routes have not been studied thoroughly yet. In addition, one of the biggest hurdles for any of these agents is the delivery

Table. IONPs Developed for Molecular Imaging of Atherosclerosis, Thrombosis, and Myocardial Infarction

Target	Size, nm	Relaxivity	Binding ligand	Target marker	Imaging modality	Ref.
Passive targeting	7	r_1=20.1 mmol/L^{-1}s^{-1} r_2=37.1 mmol/L^{-1}s^{-1}	Citrate	Macrophage-monocyte system	SGM-MRI	32
	93	…	PEG	Macrophage-monocyte system	PET NIRF	36
Macrophages and monocytes with dextran	30	r_1=15 mmol/L^{-1}s^{-1} r_2=89 mmol/L^{-1}s^{-1}	Dextran	Dextran-binding C-type lectins	MRI cine-CMR	41
	…	…	Dextran	Dextran-binding C-type lectins	Fluorescence tomography MRI	42
	30	…	Dextran	Dextran-binding C-type lectins	Digital autoradiography MRI	44
	20–30	…	Dextran	Dextran-binding C-type lectins	NIRF MRI	43
	20–150	…	Dextran and MCP-1	Dextran-binding C-type lectins and CCR2	MRI	45
Macrophages and monocytes with other moieties	7.3	r_2=135.2 mmol/L^{-1}s^{-1}	OPN antibody	Osteopontin	Fluorescence imaging MRI	47
	47	r_2=168.24 mmol/L^{-1}s^{-1}	Tenascin-C antibody	Tenascin-C	MRI	49
	HA-SPION20 HA-NW65	…	Hyaluronan	CD44	MRI	51
	6	…	CD163 antibody	CD163	MRI	53
	20	r_1=8.2 mmol/L^{-1}s^{-1} r_2=20.1 mmol/L^{-1}s^{-1}	Annexin V	Phosphatidyl-serine	SPECT MRI	55
	180	…	D-mannose PLL	Mannose receptors	MRI	57
Endothelial cells	40.6	…	E-selectin antibody	E-selectin	MRI	58,59
	404.4	…	VEGFR2 antibody	VEGFR2	Ultrasound MRI	61
Vascular smooth muscle cells	30.2	r_2=134.5 mmol/L^{-1}s^{-1}	Profilin-1 antibody	Profilin-1	NIRF MRI	63
Activated platelets	…	…	scFv	LIBS epitopes on glycoprotein IIb/IIIa	MRI	29
	7.7	r_1=5.3 mmol/L^{-1}s^{-1} r_2=73.4 mmol/L^{-1}s^{-1}	scFv	LIBS epitopes on glycoprotein IIb/IIIa	MRI	16
	7.5	r_2=273 mmol/L^{-1}s^{-1}	rIgG4 TEG4 antibody	Glycoproteins αIIB and β3	MRI	67
	33.8	r_1=37.5 mmol/L^{-1}s^{-1} r_2=137 mmol/L^{-1}s^{-1}	Fucoidan	P-selectin	MRI	69
	368	…	cRGD	Glycoprotein IIb/IIIa	MRI	71
Tissue factor	100	…	EGFP-EGF1	Tissue factor	MSFI MRI	72
Fibrin	40	r_1=5.6 mmol/L^{-1}s^{-1} r_2=207 mmol/L^{-1}s^{-1}	FibPep (Cyclic RWQPCPAESWT-Cha-CWDP)	Fibrin	MRI	74
	20–30	r_2=457 mmol/L^{-1}s^{-1}	CREKA	Fibrin	MRI	76
	160	r_1=44.6 mmol/L^{-1}s^{-1} r_2=489 mmol/L^{-1}s^{-1}	FibPep (GPRPPGGS[Lys(TMR)]GC)	Fibrin	MRI	77

CMR indicates cardiac magnetic resonance; EGFP-EGF1, fluorescent protein-epidermal growth factor 1; IONP, iron oxide nanoparticle; MCP-1, chemoattractant protein 1; MRI, magnetic resonance imaging; MSFI, multispectral fluorescence imaging; NIFR, near-infrared fluorescence; PEG, polyethylene glycol; PET, positron emission topography; PLL, poly(L-lysine); SGM-MRI, susceptibility gradient mapping magnetic resonance imaging; SPECT, single-photon-emission computed tomography; and VEGFR2, vascular endothelial growth factor receptor 2.

in enough quantities to enable imaging. Therefore, strategies for overcoming these challenges are required. By understanding these clinically observed limitations, ongoing research and clinical trials are currently being performed to design improved IONPs. As a consequence, limitations are being reduced, and clinical acceptance is expected to increase.

ARTICLE INFORMATION

Received September 26, 2020; accepted December 8, 2020.

Affiliations

Australian Institute for Bioengineering and Nanotechnology (K.X.V.-P., Z.P.X., H.T.T.) and School of Pharmacy, Pharmacy Australia Centre of Excellence (K.X.V.-P., J.L., D.K., P.J.L.), the University of Queensland, Australia. Queensland Micro- and Nanotechnology (K.X.V.-P., H.T.T.) and School of Environment and Science (H.T.T.), Griffith University, Brisbane, Australia. Department of Pharmacy, Xinhua College of Sun Yat-sen University, China (P.J.L.).

Sources of Funding

This work is funded by National Health and Medical Research Council (H.T. Ta: APP1037310, APP1182347), Heart Foundation (H.T. Ta: 102761), and the University of Queensland (K.X. Vazquez-Prada: Research Training Scholarship).

Disclosures

None.

REFERENCES

1. WHO. Cardiovascular diseases (CVDs). 2017.
2. Varna M, Juenet M, Bayles R, Mazighi M, Chauvierre C, Letourneur D. Nanomedicine as a strategy to fight thrombotic diseases. *Future Sci OA.* 2015;1:FSO46. doi: 10.4155/fso.15.46
3. Falk E. Pathogenesis of atherosclerosis. *J Am Coll Cardiol.* 2006;47(suppl 8):C7–12. doi: 10.1016/j.jacc.2005.09.068
4. Mackman N. Triggers, targets and treatments for thrombosis. *Nature.* 2008;451:914–918. doi: 10.1038/nature06797
5. Rostam MA, Kamato D, Piva TJ, Zheng W, Little PJ, Osman N. The role of specific Smad linker region phosphorylation in TGF-β mediated expression of glycosaminoglycan synthesizing enzymes in vascular smooth muscle. *Cell Signal.* 2016;28:956–966. doi: 10.1016/j.cellsig.2016.05.002
6. Sato K, Yoshizawa H, Seki T, Shirai R, Yamashita T, Okano T, Shibata K, Wakamatsu MJ, Mori Y, Morita T, et al. Chemerin-9, a potent agonist of chemerin receptor (ChemR23), prevents atherogenesis. *Clin Sci (Lond).* 2019;133:1779–1796. doi: 10.1042/CS20190336
7. Wang T, Butany J. Pathogenesis of atherosclerosis. *Diagn Histopathol.* 2017;23:473–478.
8. Yusof NNM, McCann A, Little PJ, Ta HT. Non-invasive imaging techniques for the differentiation of acute and chronic thrombosis. *Thromb Res.* 2019;177:161–171. doi: 10.1016/j.thromres.2019.03.009
9. Bentzon JF, Otsuka F, Virmani R, Falk E. Mechanisms of plaque formation and rupture. *Circ Res.* 2014;114:1852–1866. doi: 10.1161/CIRCRESAHA.114.302721
10. Nishimoto K, Mimura A, Aoki M, Banura N, Murase K. Application of magnetic particle imaging to pulmonary imaging using nebulized magnetic nanoparticles: phantom and small animal experiments. *Open J Med Imaging.* 2015;5:49–55.
11. Wadajkar AS, Santimano S, Rahimi M, Yuan B, Banerjee S, Nguyen KT. Deep vein thrombosis: current status and nanotechnology advances. *Biotechnol Adv.* 2013;31:504–513. doi: 10.1016/j.biotechadv.2012.08.004
12. Koupenova M, Kehrel BE, Corkrey HA, Freedman JE. Thrombosis and platelets: an update. *Eur Heart J.* 2017;38:785–791. doi: 10.1093/eurheartj/ehw550
13. Olaf M, Cooney R. Deep venous thrombosis. *Emerg Med Clin North Am.* 2017;35:743–770. doi: 10.1016/j.emc.2017.06.003
14. Lu L, Liu M, Sun R, Zheng Y, Zhang P. Myocardial infarction: symptoms and treatments. *Cell Biochem Biophys.* 2015;72:865–867. doi: 10.1007/s12013-015-0553-4
15. Aziz M, Yadav K. Pathogenesis of atherosclerosis. *Med Clin Rev.* 2016;2.
16. Ta HT, Li Z, Hagemeyer CE, Cowin G, Zhang S, Palasubramaniam J, Alt K, Wang X, Peter K, Whittaker AK. Molecular imaging of activated platelets via antibody-targeted ultra-small iron oxide nanoparticles displaying unique dual MRI contrast. *Biomaterials.* 2017;134:31–42. doi: 10.1016/j.biomaterials.2017.04.037
17. Tong S, Hou S, Zheng Z, Zhou J, Bao G. Coating optimization of superparamagnetic iron oxide nanoparticles for high T2 relaxivity. *Nano Lett.* 2010;10:4607–4613. doi: 10.1021/nl102623x
18. Siegel-Axel DI, Gawaz M. Platelets and endothelial cells. *Semin Thromb Hemost.* 2007;33:128–135. doi: 10.1055/s-2007-969025
19. Arndt N, Tran HD, Zhang R, Xu ZP, Ta HT. Different approaches to develop nanosensors for diagnosis of diseases. *Adv Sci.* 2020:2001476.
20. Liu Y, Wu Y, Zhang R, et al. Investigating the use of layered double hydroxide nanoparticles as carriers of metal oxides for theranostics of ROS-related diseases. *ACS Appl Bio Mater.* 2019;2:5930–5940.
21. Zhang Y, Koradia A, Kamato D, Popat A, Little PJ, Ta HT. Treatment of atherosclerotic plaque: perspectives on theranostics. *J Pharm Pharmacol.* 2019;71:1029–1043. doi: 10.1111/jphp.13092
22. Ta HT, Li Z, Hagemeyer C, et al. Novel bionanotechnological solutions based on metal oxide and metal to preserve and assess organs for transplantation. *Cryobiology.* 2018;81:233.
23. Gaston E, Fraser JF, Xu ZP, Ta HT. Nano- and micro-materials in the treatment of internal bleeding and uncontrolled hemorrhage. *Nanomedicine.* 2018;14:507–519. doi: 10.1016/j.nano.2017.11.007
24. Montiel Schneider MG, Lassalle VL. Magnetic iron oxide nanoparticles as novel and efficient tools for atherosclerosis diagnosis. *Biomed Pharmacother.* 2017;93:1098–1115. doi: 10.1016/j.biopha.2017.07.012
25. Ta HT, Li Z, Wu Y, et al. Effects of magnetic field strength and particle aggregation on relaxivity of ultra-small dual contrast iron oxide nanoparticles. *Mater Res Exp.* 2017;4:116105.
26. Ta H, Li Z, Hagemeyer C, et al. Self-confirming molecular imaging of activated platelets via iron oxide nanoparticles displaying unique dual MRI contrast. *Atherosclerosis.* 2017;263:e146.
27. Wu Y, Yang Y, Zhao, W, et al. Novel iron oxide–cerium oxide core–shell nanoparticles as a potential theranostic material for ROS related inflammatory diseases. *J Mater Chem B.* 2018;6:4937–4951.
28. Hagemeyer CE, Alt K, Johnston AP, Such GK, Ta HT, Leung MK, Prabhu S, Wang X, Caruso F, Peter K. Particle generation, functionalization and sortase A-mediated modification with targeting of single-chain antibodies for diagnostic and therapeutic use. *Nat Protoc.* 2015;10:90–105. doi: 10.1038/nprot.2014.177
29. Ta HT, Prabhu S, Leitner E, Jia F, von Elverfeldt D, Jackson KE, Heidt T, Nair AK, Pearce H, von Zur Muhlen C, et al. Enzymatic single-chain antibody tagging: a universal approach to targeted molecular imaging and cell homing in cardiovascular disease. *Circ Res.* 2011;109:365–373. doi: 10.1161/CIRCRESAHA.111.249375
30. Jacques V, Dumas S, Sun WC, Troughton JS, Greenfield MT, Caravan P. High-relaxivity magnetic resonance imaging contrast agents. Part 2. Optimization of inner- and second-sphere relaxivity. *Invest Radiol.* 2010;45:613–624. doi: 10.1097/RLI.0b013e3181ee6a49
31. Kooi ME, Cappendijk VC, Cleutjens KB, Kessels AG, Kitslaar PJ, Borgers M, Frederik PM, Daemen MJ, van Engelshoven JM. Accumulation of ultrasmall superparamagnetic particles of iron oxide in human atherosclerotic plaques can be detected by *in vivo* magnetic resonance imaging. *Circulation.* 2003;107:2453–2458. doi: 10.1161/01.CIR.0000068315.98705.CC
32. Makowski MR, Varma G, Wiethoff AJ, Smith A, Mattock K, Jansen CH, Warley A, Taupitz M, Schaeffter T, Botnar RM. Noninvasive assessment of atherosclerotic plaque progression in ApoE-/- mice using susceptibility gradient mapping. *Circ Cardiovasc Imaging.* 2011;4:295–303. doi: 10.1161/CIRCIMAGING.110.957209
33. Owens DE III, Peppas NA. Opsonization, biodistribution, and pharmacokinetics of polymeric nanoparticles. *Int J Pharm.* 2006;307:93–102. doi: 10.1016/j.ijpharm.2005.10.010
34. Suk JS, Xu Q, Kim N, Hanes J, Ensign LM. PEGylation as a strategy for improving nanoparticle-based drug and gene delivery. *Adv Drug Deliv Rev.* 2016;99(Pt A):28–51. doi: 10.1016/j.addr.2015.09.012
35. Ishida T, Kiwada H. Accelerated blood clearance (ABC) phenomenon upon repeated injection of PEGylated liposomes. *Int J Pharm.* 2008;354:56–62. doi: 10.1016/j.ijpharm.2007.11.005
36. Im HJ, England CG, Feng L, Graves SA, Hernandez R, Nickles RJ, Liu Z, Lee DS, Cho SY, Cai W. Accelerated blood clearance phenomenon reduces the passive targeting of PEGylated nanoparticles in peripheral arterial disease. *ACS Appl Mater Interfaces.* 2016;8:17955–17963. doi: 10.1021/acsami.6b05840

37. England CG, Im HJ, Feng L, Chen F, Graves SA, Hernandez R, Orbay H, Xu C, Cho SY, Nickles RJ, et al. Re-assessing the enhanced permeability and retention effect in peripheral arterial disease using radiolabeled long circulating nanoparticles. *Biomaterials.* 2016;100:101–109. doi: 10.1016/j.biomaterials.2016.05.018
38. Zia A, Wu Y, Nguyen T, Wang X, Peter K, Ta HT. The choice of targets and ligands for site-specific delivery of nanomedicine to atherosclerosis. *Cardiovasc Res.* 2020.
39. Tarudji AW, Kievit FM. Active targeting and transport. *Nanoparticles for Biomedical Applications.* Elsevier; 2020:19–36.
40. Ma L, Liu TW, Wallig MA, Dobrucki IT, Dobrucki LW, Nelson ER, Swanson KS, Smith AM. Efficient targeting of adipose tissue macrophages in obesity with polysaccharide nanocarriers. *ACS Nano.* 2016;10:6952–6962. doi: 10.1021/acsnano.6b02878
41. Yilmaz A, Dengler MA, van der Kuip H, Yildiz H, Rösch S, Klumpp S, Klingel K, Kandolf R, Helluy X, Hiller KH, et al. Imaging of myocardial infarction using ultrasmall superparamagnetic iron oxide nanoparticles: a human study using a multi-parametric cardiovascular magnetic resonance imaging approach. *Eur Heart J.* 2013;34:462–475. doi: 10.1093/eurheartj/ehs366
42. Sosnovik DE, Nahrendorf M, Deliolanis N, Novikov M, Aikawa E, Josephson L, Rosenzweig A, Weissleder R, Ntziachristos V. Fluorescence tomography and magnetic resonance imaging of myocardial macrophage infiltration in infarcted myocardium in vivo. *Circulation.* 2007;115:1384–1391. doi: 10.1161/CIRCULATIONAHA.106.663351
43. Stein-Merlob AF, Hara T, McCarthy JR, Mauskapf A, Hamilton JA, Ntziachristos V, Libby P, Jaffer FA. Atheroma susceptible to thrombosis exhibit impaired endothelial permeability in vivo as assessed by nanoparticle-based fluorescence molecular imaging. *Circ Cardiovasc Imaging.* 2017;10:85–92.
44. de Barros AL, Chacko AM, Mikitsh JL, Al Zaki A, Salavati A, Saboury B, Tsourkas A, Alavi A. Assessment of global cardiac uptake of radiolabeled iron oxide nanoparticles in apolipoprotein-E-deficient mice: implications for imaging cardiovascular inflammation. *Mol Imaging Biol.* 2014;16:330–339. doi: 10.1007/s11307-013-0709-9
45. Kao CW, Wu PT, Liao MY, Chung IJ, Yang KC, Isaac Tseng WY, Yu J. Magnetic nanoparticles conjugated with peptides derived from monocyte chemoattractant protein-1 as a tool for targeting atherosclerosis. *Pharmaceutics.* 2018;10:62–79.
46. Bidder M, Shao JS, Charlton-Kachigian N, Loewy AP, Semenkovich CF, Towler DA. Osteopontin transcription in aortic vascular smooth muscle cells is controlled by glucose-regulated upstream stimulatory factor and activator protein-1 activities. *J Biol Chem.* 2002;277:44485–44496. doi: 10.1074/jbc.M206235200
47. Qiao H, Wang Y, Zhang R, Gao Q, Liang X, Gao L, Jiang Z, Qiao R, Han D, Zhang Y, et al. MRI/optical dual-modality imaging of vulnerable atherosclerotic plaque with an osteopontin-targeted probe based on Fe3O4 nanoparticles. *Biomaterials.* 2017;112:336–345. doi: 10.1016/j.biomaterials.2016.10.011
48. Liu R, He Y, Li B, Liu J, Ren Y, Han W, Wang X, Zhang L. Tenascin-C produced by oxidized LDL-stimulated macrophages increases foam cell formation through Toll-like receptor-4. *Mol Cells.* 2012;34:35–41. doi: 10.1007/s10059-012-0054-x
49. Li Y, Liu J, Huang JW, Song JC, Ma ZL, Shi HB. *In vivo* MRI detection of atherosclerosis in ApoE-deficient mice by using tenascin-C-targeted USPIO. *Acta Radiol.* 2018;59:1431–1437. doi: 10.1177/0284185118762613
50. Vendrov AE, Madamanchi NR, Niu XL, Molnar KC, Runge M, Szyndralewiez C, Page P, Runge MS. NADPH oxidases regulate CD44 and hyaluronic acid expression in thrombin-treated vascular smooth muscle cells and in atherosclerosis. *J Biol Chem.* 2010;285:26545–26557. doi: 10.1074/jbc.M110.143917
51. Hossaini Nasr S, Tonson A, El-Dakdouki MH, Zhu DC, Agnew D, Wiseman R, Qian C, Huang X. Effects of nanoprobe morphology on cellular binding and inflammatory responses: hyaluronan-conjugated magnetic nanoworms for magnetic resonance imaging of atherosclerotic plaques. *ACS Appl Mater Interfaces.* 2018;10:11495–11507. doi: 10.1021/acsami.7b19708
52. Ta HT, Truong NP, Whittaker AK, Davis TP, Peter K. The effects of particle size, shape, density and flow characteristics on particle margination to vascular walls in cardiovascular diseases. *Expert Opin Drug Deliv.* 2018;15:33–45. doi: 10.1080/17425247.2017.1316262
53. Tarin C, Carril M, Martin-Ventura JL, Markuerkiaga I, Padro D, Llamas-Granda P, Moreno JA, García I, Genicio N, Plaza-Garcia S, et al. Targeted gold-coated iron oxide nanoparticles for CD163 detection in atherosclerosis by MRI. *Sci Rep.* 2015;5:17135. doi: 10.1038/srep17135
54. Kolodgie FD, Petrov A, Virmani R, Narula N, Verjans JW, Weber DK, Hartung D, Steinmetz N, Vanderheyden JL, Vannan MA, et al. Targeting of apoptotic macrophages and experimental atheroma with radiolabeled annexin V: a technique with potential for noninvasive imaging of vulnerable plaque. *Circulation.* 2003;108:3134–3139. doi: 10.1161/01.CIR.0000105761.00573.50
55. Cheng D, Li X, Zhang C, Tan H, Wang C, Pang L, Shi H. Detection of vulnerable atherosclerosis plaques with a dual-modal single-photon-emission computed tomography/magnetic resonance imaging probe targeting apoptotic macrophages. *ACS Appl Mater Interfaces.* 2015;7:2847–2855. doi: 10.1021/am508118x
56. Varasteh Z, Mohanta S, Li Y, López Armbruster N, Braeuer M, Nekolla SG, Habenicht A, Sager HB, Raes G, Weber W, et al. Targeting mannose receptor expression on macrophages in atherosclerotic plaques of apolipoprotein E-knockout mice using 68 Ga-NOTA-anti-MMR nanobody: non-invasive imaging of atherosclerotic plaques. *EJNMMI Res.* 2019;9:40–45.
57. Babič M, Schmiedtová M, Poledne R, Herynek V, Horák D. In vivo monitoring of rat macrophages labeled with poly(l-lysine)-iron oxide nanoparticles. *J Biomed Mater Res B.* 2015;103:1141–1148.
58. Kang HW, Josephson L, Petrovsky A, Weissleder R, Bogdanov A Jr. Magnetic resonance imaging of inducible E-selectin expression in human endothelial cell culture. *Bioconjug Chem.* 2002;13:122–127. doi: 10.1021/bc0155521
59. Kang HW, Torres D, Wald L, Weissleder R, Bogdanov AA Jr. Targeted imaging of human endothelial-specific marker in a model of adoptive cell transfer. *Lab Invest.* 2006;86:599–609. doi: 10.1038/labinvest.3700421
60. Camaré C, Pucelle M, Nègre-Salvayre A, Salvayre R. Angiogenesis in the atherosclerotic plaque. *Redox Biol.* 2017;12:18–34. doi: 10.1016/j.redox.2017.01.007
61. Chen H, Chen L, Liang R, Wei J. Ultrasound and magnetic resonance molecular imaging of atherosclerotic neovasculature with perfluorocarbon magnetic nanocapsules targeted against vascular endothelial growth factor receptor 2 in rats. *Mol Med Rep.* 2017;16:5986–5996. doi: 10.3892/mmr.2017.7314
62. Peterson SM, Turner JE, Harrington A, Davis-Knowlton J, Lindner V, Gridley T, Vary CPH, Liaw L. Notch2 and proteomic signatures in mouse neointimal lesion formation. *Arterioscler Thromb Vasc Biol.* 2018;38:1576–1593. doi: 10.1161/ATVBAHA.118.311092
63. Wang Y, Chen J, Yang B, Qiao H, Gao L, Su T, Ma S, Zhang X, Li X, Liu G, et al. *In vivo* MR and fluorescence dual-modality imaging of atherosclerosis characteristics in mice using profilin-1 targeted magnetic nanoparticles. *Theranostics.* 2016;6:272–286. doi: 10.7150/thno.13350
64. Ta HT, Prabhu S, Leitner EE, et al. Targeted molecular imaging and cell homing in cardiovascular disease via antibody-sortagging. *Atherosclerosis.* 2015;241:e26.
65. Ta HT, Peter K, Hagemeyer CE. Enzymatic antibody tagging: toward a universal biocompatible targeting tool. *Trends Cardiovasc Med.* 2012;22:105–111. doi: 10.1016/j.tcm.2012.07.004
66. Ta HT, Prabhu S, Leitner E, et al. Antibody-sortagging: a universal approach towards targeted molecular imaging and cell homing in cardiovascular disease. *Circ Res.* 2010;107:e37–e38.
67. Jacobin-Valat MJ, Laroche-Traineau J, Larivière M, Mornet S, Sanchez S, Biran M, Lebaron C, Boudon J, Lacomme S, Cérutti M, et al. Nanoparticles functionalised with an anti-platelet human antibody for *in vivo* detection of atherosclerotic plaque by magnetic resonance imaging. *Nanomedicine.* 2015;11:927–937. doi: 10.1016/j.nano.2014.12.006
68. Bachelet L, Bertholon I, Lavigne D, Vassy R, Jandrot-Perrus M, Chaubet F, Letourneur D. Affinity of low molecular weight fucoidan for P-selectin triggers its binding to activated human platelets. *Biochim Biophys Acta.* 2009;1790:141–146. doi: 10.1016/j.bbagen.2008.10.008
69. Suzuki M, Bachelet-Violette L, Rouzet F, Beilvert A, Autret G, Maire M, Menager C, Louedec L, Choqueux C, Sabboural P, et al. Ultrasmall superparamagnetic iron oxide nanoparticles coated with fucoidan for molecular MRI of intraluminal thrombus. *Nanomedicine (Lond).* 2015;10:73–87. doi: 10.2217/nnm.14.51
70. Smith LL, Cheung HK, Ling LE, Chen J, Sheppard D, Pytela R, Giachelli CM. Osteopontin N-terminal domain contains a cryptic adhesive sequence recognized by alpha9beta1 integrin. *J Biol Chem.* 1996;271:28485–28491.
71. Liu J, Xu J, Zhou J, Zhang Y, Guo D, Wang Z. Fe3O4-based PLGA nanoparticles as MR contrast agents for the detection of thrombosis. *Int J Nanomedicine.* 2017;12:1113–1126. doi: 10.2147/IJN.S123228
72. Hu Y, Li Z, Shi W, Yin Y, Mei H, Wang H, Guo T, Deng J, Yan H, Lu X. Early diagnosis of cerebral thrombosis by EGFP-EGF1 protein conjugated ferroferric oxide magnetic nanoparticles. *J Biomater Appl.* 2019;33:1195–1201. doi: 10.1177/0885328218823475

73. Mori H, Kolodgie FD, Finn AV, Virmani R. Pathology and pathophysiology of coronary atherosclerotic plaques. *CT of the Heart*. Springer; 2019:211–226.
74. Starmans LW, Moonen RP, Aussems-Custers E, Daemen MJ, Strijkers GJ, Nicolay K, Grüll H. Evaluation of iron oxide nanoparticle micelles for magnetic particle imaging (MPI) of thrombosis. *PLoS One*. 2015;10:e0119257. doi: 10.1371/journal.pone.0119257
75. Stefanelli VL, Barker TH. The evolution of fibrin-specific targeting strategies. *J Mater Chem B*. 2015;3:1177–1186. doi: 10.1039/C4TB01769B
76. Poon C, Gallo J, Joo J, Chang T, Bañobre-López M, Chung EJ. Hybrid, metal oxide-peptide amphiphile micelles for molecular magnetic resonance imaging of atherosclerosis. *J Nanobiotechnology*. 2018;16:92. doi: 10.1186/s12951-018-0420-8
77. Ta HT, Arndt N, Wu Y, Lim HJ, Landeen S, Zhang R, Kamato D, Little PJ, Whittaker AK, Xu ZP. Activatable magnetic resonance nanosensor as a potential imaging agent for detecting and discriminating thrombosis. *Nanoscale*. 2018;10:15103–15115. doi: 10.1039/c8nr05095c
78. Ta HT. Activatable magnetic resonance nanosensor as a potential imaging agent for detecting and discriminating thrombosis. *Atherosclerosis*. 2019;32:159.
79. Yang K, Hu L, Ma X, Ye S, Cheng L, Shi X, Li C, Li Y, Liu Z. Multimodal imaging guided photothermal therapy using functionalized graphene nanosheets anchored with magnetic nanoparticles. *Adv Mater*. 2012;24:1868–1872. doi: 10.1002/adma.201104964
80. Liu H, Chen X, Xue W, Chu C, Liu Y, Tong H, Du X, Xie T, Liu G, Zhang W. Recombinant epidermal growth factor-like domain-1 from coagulation factor VII functionalized iron oxide nanoparticles for targeted glioma magnetic resonance imaging. *Int J Nanomedicine*. 2016;11:5099–5108. doi: 10.2147/IJN.S116980
81. Anselmo AC, Mitragotri S. Nanoparticles in the clinic. *Bioeng Transl Med*. 2016;1:10–29. doi: 10.1002/btm2.10003
82. Anselmo AC, Mitragotri S. Nanoparticles in the clinic: an update. *Bioeng Transl Med*. 2019;4:e10143. doi: 10.1002/btm2.10143
83. Wang YX. Current status of superparamagnetic iron oxide contrast agents for liver magnetic resonance imaging. *World J Gastroenterol*. 2015;21:13400–13402. doi: 10.3748/wjg.v21.i47.13400
84. Toth GB, Varallyay CG, Horvath A, Bashir MR, Choyke PL, Daldrup-Link HE, Dosa E, Finn JP, Gahramanov S, Harisinghani M, et al. Current and potential imaging applications of ferumoxytol for magnetic resonance imaging. *Kidney Int*. 2017;92:47–66. doi: 10.1016/j.kint.2016.12.037